J Petrol Explor Prod Technol (2018) 8:17–30
https://doi.org/10.1007/s13202-017-0316-4

ORIGINAL PAPER - PRODUCTION ENGINEERING

Development of a new correlation to determine the static Young's modulus

Salaheldin Elkatatny[1] · Mohamed Mahmoud[1] · Ibrahim Mohamed[2] · Abdulazeez Abdulraheem[1]

Received: 23 September 2016 / Accepted: 5 January 2017 / Published online: 30 January 2017

Abstract The estimation of the in situ stresses is very crucial in oil and gas industry applications. Prior knowledge of the in situ stresses is essential in the design of hydraulic fracturing operations in conventional and unconventional reservoirs. The fracture propagation and fracture mapping are strong functions of the values and directions of the in situ stresses. Other applications such as drilling require the knowledge of the in situ stresses to avoid the wellbore instability problems. The estimation of the in situ stresses requires the knowledge of the Static Young's modulus of the rock. Young's modulus can be determined using expensive techniques by measuring the Young's modulus on actual cores in the laboratory. The laboratory values are then used to correlate the dynamic values derived from the logs. Several correlations were introduced in the literature, but those correlations were very specific and when applied to different cases they gave very high errors and were limited to relating the dynamic Young' modulus with the log data. The objective of this paper is to develop an accurate and robust correlation for static Young's modulus to be estimated directly from log data without the need for core measurements. Multiple regression analysis was performed on actual core and log data using 600 data points to develop the new correlations. The static Young's modulus was found to be a strong function on three log parameters, namely compressional transit time, shear transit time, and bulk density. The new correlation was tested for different cases with different lithology such as calcite, dolomite, and sandstone. It gave good match to the measured data in the laboratory which indicates the accuracy and robustness of this correlation. In addition, it outperformed all correlations from the literature in predicting the static Young's modulus. It will also help in saving time as well as cost because only the available log data are used in the prediction.

Keywords Static Young's modulus · Dynamic Young's modulus · Log data · Hydraulic fracturing · In situ stresses · Correlation

List of symbols

E	Young's modulus
Δt	Transit time
ε	Strain
ν	Poisson's ratio
ρ_b	Bulk density of the rock
σ	Stress

Subscripts

s	Shear
p	Compressional
dynamic	Dynamic value
static	Static value

Introduction

The terms Young's modulus, tensile modulus, elastic modulus, modulus of elasticity, and stiffness are refereeing to the mechanical property that measures the stiffness of a certain material. Young's modulus is the ratio of the stress applied on the material to strain associated with the applied

✉ Salaheldin Elkatatny
elkatatny@kfupm.edu.sa

[1] King Fahd University of Petroleum and Minerals, Dhahran, Saudi Arabia

[2] Advantek Waste Management Services, Houston, TX, USA

stress (Chen 2011). Young's Modulus can be calculated using Hook's Law (Nguyen et al. 2009) as follows:

$$E = \frac{\sigma}{\varepsilon} \quad (1)$$

where E = Young's modulus (GPa), σ = stress (GPa), and ε = strain.

Young's modulus is different for different rock type; the value depends on the rock properties including porosity, lithology, temperature, pore pressure, fluid saturation, and the rock consolidation (William 1969). Soft formations like shale have a low Young's modulus value (100,000–1,000,000 psi) comparing to medium formations like sandstone (2,000,000–10,000,000) and hard formation limestone (8,000,000–12,000,000 psi) as presented by Nur and Wang (1989).

The ranges presented above show that there is no typical value of Young's modulus for certain rock, and measuring the Young's modulus is a must in order to conduct the geomechanical analysis for the formation in interest. Building a geomechanical model is essential for several applications related to mechanical rock failure during well drilling, completion, and stimulation, which include estimation of the formation breakdown pressure, fracture simulation, wellbore stability, and formation compaction (Ciccotti and Mulargia 2004).

Young's Modulus can be either calculated from the sonic and density logs (dynamic Young's modulus), or measured directly in the laboratory (static Young's modulus). The dynamic modulus is usually significantly higher than the static moduli as originally noted by Zisman (1933) and Idle (1936). The difference between the dynamic and static modulus is more pronounced for soft rocks (sandstone) than hard rock (granite) (King 1966).

Idel (1936), Brace (1965), and Walsh (1966) stated that the difference between the static and dynamic modulus is strongly affected by the rock microstructure (natural fractures and pores) and the confining stress. High stresses might close the microcracks and result in increase in the velocity waves as the rock is compacted. The faster waves will be interpreted as a higher elastic modulus (dynamic modulus). Zisman (1933) explained the difference between the static and dynamic modulus by the loss of energy that the wave pulse might suffer when passing through the rock pores (intergranular pores or natural fractures) due to reflection and refraction at the fluid/rock interfaces (Howarth 1984). Static Young's modulus is often used in the wellbore stability and in situ stress applications (Ledbetter 1993; Hammam and Eliwa 2013). However, collecting cores from the well to measure the moduli in the laboratory is expensive and usually not feasible.

Several equations have been developed to establish a relationship between the static and dynamic Young's modulus. However, the applicability of each of those correlations is limited to specific rock type under certain conditions. Belikov et al. (1970) has developed a correlation to estimate the static Young's modulus from the dynamic one. However, his equation is only applicable for microcline and granite rock. King (1983) established a correlation for igneous and metamorphic rocks. McCann and Entwisle (1992) equation is valid for Jurassic granites. Morales and Marcinew (1993) correlation can be used for rocks with high permeability values. Wang (2000) has developed two different correlations for hard and soft rocks. Gorjainov (1979) introduced two relationships for clays and for wet soils. Also, there are some other equations that can be used for a wide range of rocks (Eissa and Kazi 1988; Canady 2010). As the Young's modulus value are strongly dependent on the rock microstructure, mineralogy, and confining stresses, neither of the correlation mentioned above give an acceptable match to the laboratory measurement for carbonate formation in Saudi Arabia as well be shown later in "Triaxial testing" section, and development of a new correlation to calculate static modulus is essential.

The in situ stresses can be determined from the leak-off test, and the fracture pressure of the formation behind the casing can be determined as well as the minimum horizontal principal stress. The nonlinear behavior of the leak-off test could be due to drilling fluid loss to the formation, fractures and cracks in the cement behind the casing (test run before cement setting), and plastic fracturing around the wellbore. The linear behavior during the leak-off test resulted from the drilling fluid compression and wellbore expansion around the well. The leak-off test should be repeated several times to distinguish between the different mechanisms to identify the rock fracture pressure and minimum horizontal stress (Zhou and Wojtanowicz 2002).

The determination of in situ stresses are important during the drilling operations to maintain the hole integrity and wellbore stability to avoid drilling problems. Integrated rock mechanical properties analysis will enhance the drilling process because rock mechanical properties are one of the groups that should be integrated with petrophysical parameters and other parameter to enhance the drilling and avoid wellbore stability problems. Nes et al. (2012) have done a complete analysis by integrating several rock and fluid properties among them is the rock mechanical parameters to reduce the wellbore stability issues during drilling using different types of drilling fluids. They developed a model that can be used to identify the drilling problems and to design the drilling operations. They used their model in high-pressure high-temperature drilling and compared the data to the field observations.

The static Young's modulus is used to identify the down hole stresses profiles which are important for fracture

mapping and fracture design in several rocks such as carbonates and unconventional shales. Li et al. (2014) introduced analytical solution to the stresses induced during the fracturing of unconventional shale and how they can be used in shale gas exploration. Their model can be used to predict the induced stresses due to the fracturing operations and also to predict the minimum spacing between the fractures to prevent the communication between these fractures which will cause loss of gas production due to the interference between these fractures. Zhou et al. (2015) studied the interaction between the hydraulic fractures in shale formations numerically. They concluded that a stress shadow area around the fracture will be generated due to the induced stresses, three areas of compressive stress will be formed, and this will affect the fracture orientation from the normal trends or directions.

Chan and Board (2009) used finite elements calculations to determine the induced stresses to heating and thermal effects. They found out that the in situ induced stresses due to thermal heating and the rock displacement are primarily affected by the temperature relation with the rock thermal expansion coefficient. They considered this coefficient to be the main factor that controls the prediction of the rock stresses.

Based on the literature survey, it can be said that till now there is no such general equation to calculate the static Young's modulus from the well log data. All the correlations reported in the literature are based on the laboratory measurements to develop the relation between dynamic and static Young' modulus which is time-consuming and expensive. The relationship should be picked carefully to satisfy the validation conditions of each equation. Otherwise, generalization will always give the wrong answer. The objective of this study is to develop a new correlation to estimate the static Young's modulus from the well log data for carbonate rocks (limestone and dolomite). This correlation can be used directly to estimate the static Young's modulus from log data (density, compressional, and shear transit times).

Triaxial testing

In the laboratory, Young's modulus can be calculated from the stress–strain curve, and the experiment can be conducted under uniaxial or triaxial stress conditions. It is always preferred to run the test under triaxial conditions because uniaxial test might overestimate the static Young's modulus value due to closing the fractures parallel to the stress direction (Thill and Peng 1974). The triaxial test is used to measure the mechanical properties of a cylindrical rock sample. The fluid pore pressure, drainage conditions, axial load, and confining stresses can be controlled to simulate the actual formation conditions.

A triaxial test is conducted by loading the sample axially while applying a constant all-around (cell or confining) pressure equivalent to the effective reservoir pressure. The prepared samples were 3.81 cm in diameter and 7.62 cm long. The end faces of all samples were cut and ground parallel. The samples were then cleaned using toluene and were vacuum-dried in the oven at 60 °C. All samples were tested under dry condition. The testing was conducted under room temperature, and confining pressure was kept constant during the loading phase. The confining pressure was calculated using Eq. (2).

$$\sigma_3' = \left(\frac{v}{1-v}\right)\left(\sigma_v - \alpha P_p\right) + \sigma_{\text{tectonic}} \quad (2)$$

where σ_3' is the effective confining pressure; v is the Poisson's ratio (assumed 0.3); σ_v is the vertical stress; α is Biot's constant (assumed 1); and P_p is the pore pressure. Tectonic component is estimated using leak-off or micro-frac tests conducted in the field.

The confining pressure was increased gradually from 0 to the required level with an increment of 0.02068 MPa/s. For the determination of E and v of the rock sample, the sample was jacketed using heat shrink tubing. The jacketed sample was then placed between the hardened steel plates, and the sample was tightly secured with the platens using steel wires. The sample was then instrumented with LVDTs (Linear Variable Differential Transformer). Two LVDTs were used for recording axial displacement. These two LVDTs were mounted on the steel platens opposite to each other using LVDT holders. The radial displacement was recorded using an LVDT mounted directly on the sample. An LVDT—instrumented rock sample is shown in

Fig. 1 A rock sample instrumented with LVDTs for measuring deformation in the sample

Fig. 1. The stress–strain response was plotted for all tested samples, and the elastic constants (Young's modulus and Poisson's ratio) were computed at 50% of the peak stress (for example, it will be at 80 MPa for Fig. 2). A tangent will be done at stress = 80 MPa, and the static Young's modulus will be calculated from the slope of the stress–strain line tangent at 80 MPa. The left curve (radial one) the slope of the tangent at 80 MPa will yield the static Young's modulus divided by the static Poisson's ratio.

Correlation development

Formation characterization

The selected formation comprising of carbonates and anhydrite. The overall petrographic characteristics of seven samples showed that the studied section is divided into three units: dolomitized grainstone, lime mudstone, and peloidal bioclastic–intraclastic dolograinstone.

Dolomitized grainstone facies were observed in two samples that consist of medium-to-coarse-grained, moderately sorted grainstone. All the matrix and debris were dolomitized showing dolomitized rhombs, Fig. 3. The grainstone was partly leached and shows both intercrystalline and intracrystalline porosity, which ranges from 9 to 10%.

The lime mudstone facies were observed in three samples consisting of gray colored compact limestone with scattered dolomite rhombs and anhydrite, Fig. 4. The rock is very tight, and the porosity ranges from 0.5 to 1.0%.

Peloidal bioclastic–intraclastic dolograinstone facies were observed in two samples consisting of medium-to-fine-grained peloidal grainstone with some skeletal debris and intraclast, Fig. 5. At some places, anhydrite is found replacing some of the leached peloidal and skeletal grains. Leaching of the grains has resulted in good porosity development, which ranges from 9 to 10%.

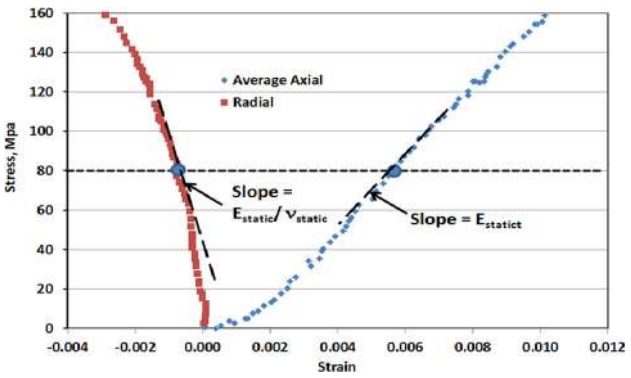

Fig. 2 Determination of static Young's modulus from stress–strain curves. E_{static} = static Young's modulus and ν_{static} = static Poisson's ratio

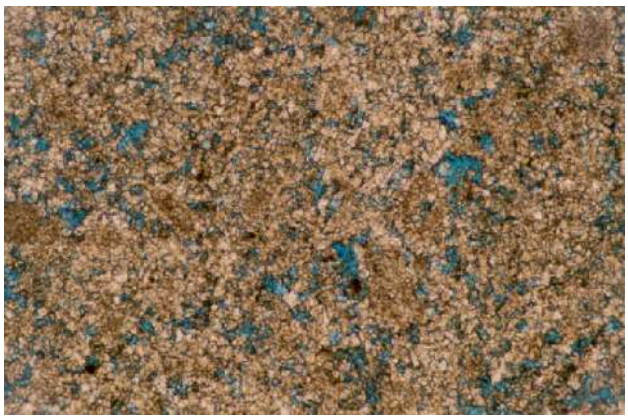

Fig. 3 Thin section photomicrograph, X25 under cross-polarized light, of carbonate sample (Depth: XX43.8 m)

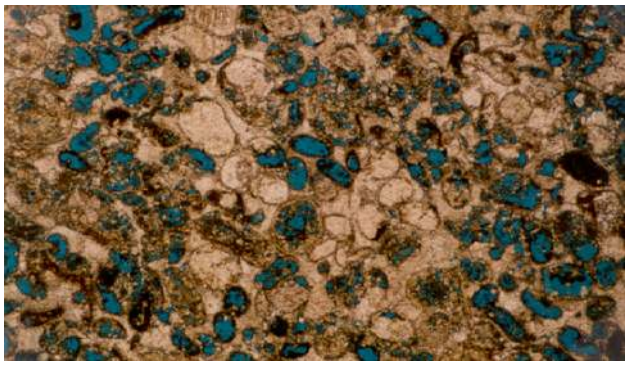

Fig. 4 Thin section photomicrograph, X25 under cross-polarized light, of carbonate sample (Depth: XX33.2 m)

Fig. 5 Thin section photomicrograph, X25 under cross-polarized light, of carbonate sample (Depth: XX44.4 m)

Log data analysis

Figure 6 shows the available log data for the selected formation. The data contain the neutron porosity, bulk density, and sonic time (compressional and shear times). The available data were used to estimate the dynamic parameters; Poisson's ratio, and Young's modulus. Figure 6 shows the results of the dynamic geomechanical

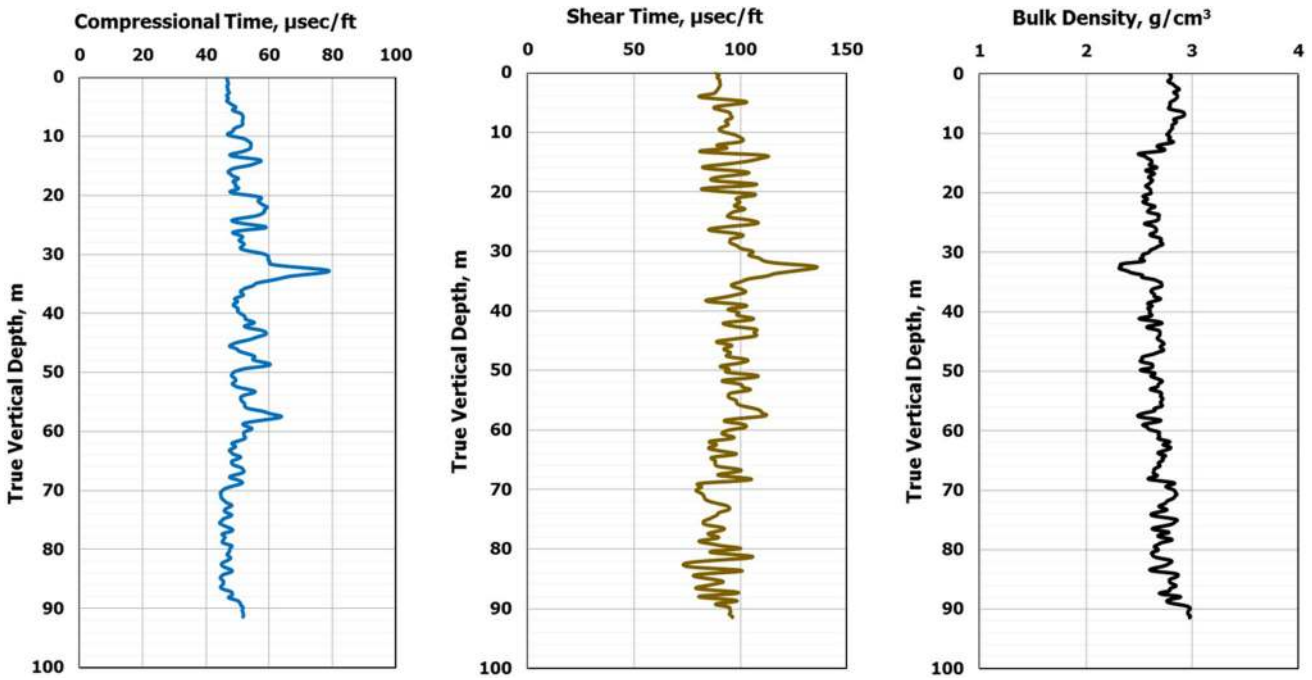

Fig. 6 Log data for the base case. The *top* depth of the formation is represented by the zero value here, and the *bottom* depth is the 91.44 m

parameters Young's Modulus (E_{dynamic}) and Poisson's Ratio (v_{dynamic}).

$$v_{\text{dynamic}} = \frac{2 - \left(\frac{\Delta t_s}{\Delta t_p}\right)^2}{2 - \left[2\left(\frac{\Delta t_s}{\Delta t_p}\right)\right]^2} \tag{3}$$

$$E_{\text{dynamic}} = 2\left(1 - v_{\text{dynamic}}\right)\left(1000\rho_b\right)\left[1000\left(\frac{0.3048}{\Delta t_s}\right)^2\right] \tag{4}$$

where Δt_s = Shear transit time, µsec/ft, Δt_p = compressional transit time, µsec/ft, ρ_b = bulk density, g/cc, v_{dynamic} = dynamic Poisson's ratio, dimensionless, E_{dynamic} = dynamic Young's Modulus, GPa.

Environmental corrections

The environmental corrections for bulk density, neutron porosity, and sonic time were performed. Corrections such mud cake correction and lithology correction were applied for all logs used. The lithology correction was done using the cross-plot.

Depth shifting

The log parameters for each static Young's modulus measured in the laboratory were obtained at the corresponding core depth after adjusting the depth between the log and core data (depth shifting). This correction of depth shift is necessary, as the depth measurement for log values using cables is not the same as that measured from the number of drill strings and core lengths for core data. Core porosity values were also used to estimate the depth shift by comparing them with the corresponding log porosity and density values. From the core and log porosity profiles, it is clarified that the coring depth shift was 1.46 m for the base case, and the core depth was increased by this value to match the log depth. Hence, no depth shift was applied to convert laboratory-based sample depth to corresponding log depth. This was done for all cases tested using the new correlation.

Static Young's modulus

Table 1 lists the static Young's modulus for five core samples that were measured in the laboratory. To obtain the static Young's modulus for all the depth range, a

Table 1 Core depth and static Young's modulus from laboratory measurements

True vertical depth (m)	E_{static} (GPa)
XX35	36
XX41	37
XX45	31
XX46	26
XX51	35

Table 2 Log data and Young's modulus (static and dynamic) values for the five core samples

TVD (m)	Δt_p (μsec/ft)	Δt_s (μsec/ft)	ρ_b (g/cm^3)	$E_{dynamic}$ (GPa)	E_{Static} (GPa)
XX35	58	100	2.61	60	36
XX41	52	99	2.65	65	37
XX45	70	121	2.46	39	31
XX46	66	116	2.51	44	26
XX51	50	101	2.60	64	35

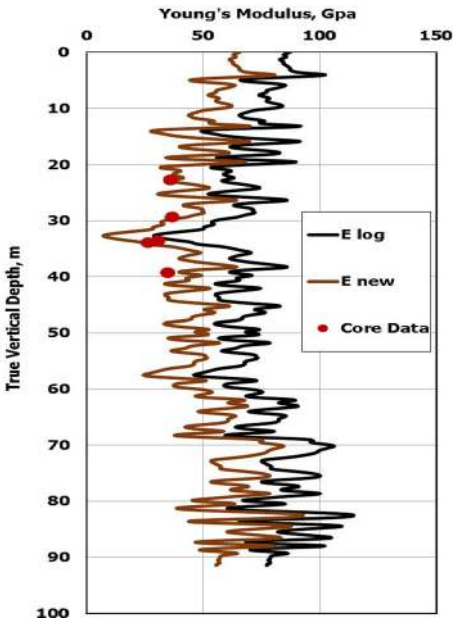

Fig. 7 Static Young's modulus calibration using regression technique

relation between dynamic Young's modulus and static Young's modulus for the five samples should be developed, and it will be used to determine the static Young's modulus profile from the log data. Table 2 lists the log value of the five samples and Young's modulus values (static and dynamic).

Regression analysis technique (Ahmed et al. 1991) was applied to calibrate the static Young's modulus with the dynamic Young's modulus. This technique is based on empirical, least-square-based curve fitting method. This technique involves two steps, first a transfer function between the static and dynamic values (log derived) is obtained by cross-plotting and curve fitting procedures, and second the transfer function is then used to calibrate the dynamic log values.

Figure 7 shows the calibration of static Young's modulus over the depth range. This method of calibration shows good match with the available core data.

New Young's modulus correlation development

In this section, a complete data analysis using correlation analysis, multiple linear regression analysis, and outlier analysis will be used in order to obtain the new correlation between Static Young's modulus and the log data from the base case. The association among variables (different log parameters) via computing correlation coefficient such as Pearson correlation coefficient, which is one of the most widely used metrics of communicating the strength of the connections between metric variables, will be analyzed. Pearson correlation coefficient value is between −1 and 1, the closer to 1 or −1, the stronger is the relationship between variables. Zero value means there is no relationship between variables.

Based on Pearson technique, the correlation coefficients between Young's modulus and compressional transit time is −0.826, and the correlation coefficients between the Young's modulus and shear transit time is −0.933. This is fairly close to −1 which suggests good correlation between Young's modulus and both compressional and shear transit times. Finally, the correlation coefficient between Young's modulus and bulk density was 0.75 which is close to 1 that indicates good relation between the two parameters.

Correlation analysis shows association among Young's modulus and log parameters such as compressional and shear transit times and bulk density of the rock. Multiple linear regression analysis predicts the type of association between variables. Multiple linear regression analysis is the process of creating a model that helps predict an unknown dependent variable y using two or more different independent variables ⟨x_1, x_2,…⟩. The following general equation should be used in order to predict the form that association takes:

$$y\_i = \beta\_0 + (\beta\_1)(x\_1) + (\beta\_2)(x\_2) + \cdots + \varepsilon\_i, \quad i = 1, \ldots, n \tag{5}$$

Outliers can affect the accuracy and the precision of the predicted model, as they tend to pull the model toward them and away from other points. Therefore, outlier analysis is needed in order to detect outliers and remove them before prediction of the model using multiple regression analysis. These outliers could weaken the model and make it less accurate. Having these points removed can improve the results of the predictions and improve the distribution of a variable.

The log data, bulk density (RHOB), shear transit time (DTS), compressional transit time (DTC), and the static Young's modulus data were presented in Fig. 8 as a series of vertically scaled parallel bars. The values of all parameters are scattered randomly in the horizontal direction (one-dimensional scatter plot). The original log data and static Young's modulus data have different data

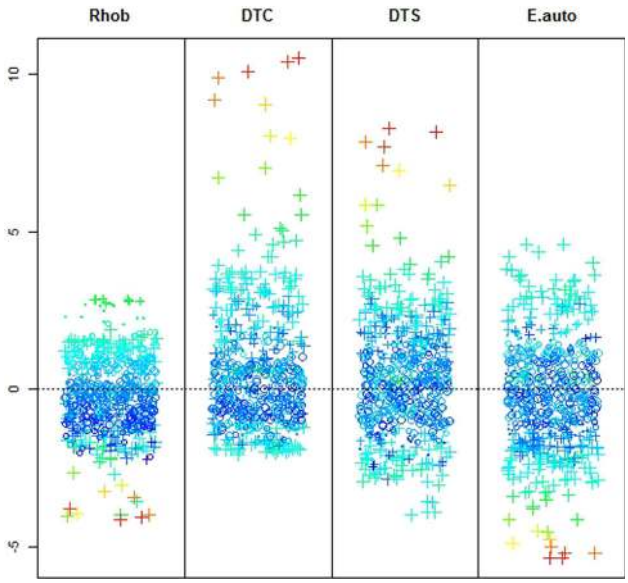

Fig. 8 Plot of single elements for the data used in the prediction of the static Young's modulus from log data

ranges; therefore, the data were first centered and scaled in the plot using the robust multivariate estimates of location and scatter. In this way, the different variables can be easily compared. This plot provides insight into the data structure and quality. Different symbols (cross means big value, circle means little value) according to the robust Mahalanobis distance based on the MCD (Minimum Covariance Determinant) estimator and different colors (red means big value, blue means little value) according to the Euclidean distances of the observations are used. Mahalanobis' distance identifies observations that are away from the center of the data cloud, giving less weight to variables with large variances or to groups of highly correlated variables (Hardin and Rocke 2005). This distance is usually preferred over the Euclidean distance which neglects the covariance structure, and all variables are treated equally. In this study, R-project statistical software was used to identify the outliers using these methods.

We used R-project to produce a multiple linear regression analysis of the training data with Young's modulus as a dependent variable and compressional and shear transit times and bulk density as the independent variables. The relative importance (dependence of Young's modulus on the parameter) between the static Young's modulus and the log parameters (compressional and shear times and bulk density). It is very clear that there is high degree of importance between shear transit time and static Young's modulus. Other log parameters were not considered because they showed very low relative importance compared to the three parameters in Fig. 9. We obtained the following correlation with 99.96 regression coefficient after removing the outliers:

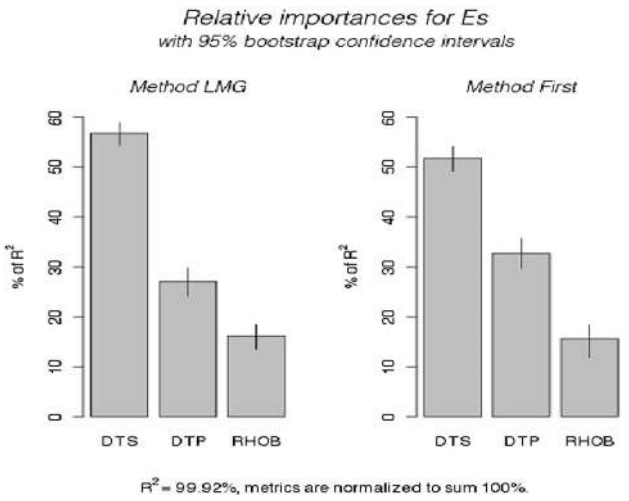

Fig. 9 Relative importance between static Young's modulus and log data

$$\ln E_{\text{static}} = 14.9 - 0.61\ln(\Delta t_{\text{p}}) - 2.18\ln(\Delta t_{\text{s}}) + 1.42\ln\rho_{\text{b}} \quad (6)$$

Estimation of static Young's modulus

Canady (2010) proposed an empirical correlation to determine static Young's modulus from dynamic Young's modulus over a wide range of rock strength and properties (Eq. 7) Wang (2000) stated that for hard rock, static Young's modulus could be determined from dynamic Young's modulus by Eq. (8). King (1983) stated that for igneous metamorphic rock, the static Young's modulus is a function of dynamic one as shown in Eq. (9). For a wide range of rock, the static Young's modulus can be determined as a function of dynamic one using Eq. (10), Eissa and Kazi (1988).

$$E_{\text{static}} = \frac{\ln(E_{\text{dynamic}} + 1)(E_{\text{dynamic}} - 1)}{4.5} \quad (7)$$

$$E_{\text{static}} = E_{\text{dynamic}} - 15.2 \quad (8)$$

$$E_{\text{static}} = 1.263E_{\text{dynamic}} - 29.5 \quad (9)$$

$$E_{\text{static}} = 0.061E_{\text{dynamic}} - 0.00258 \quad (10)$$

Validation of the new correlation

Four different cases were used to validate the developed correlation involving data that were not used for calibration or training. The results are compared with the available correlations in the literature, as described below.

Case #1

The reservoir section of this case is limestone formation, and the available log data are shown in Fig. 10. Seven core data, which obtained from triaxle test, are available for checking the accuracy of estimated value of static Young's

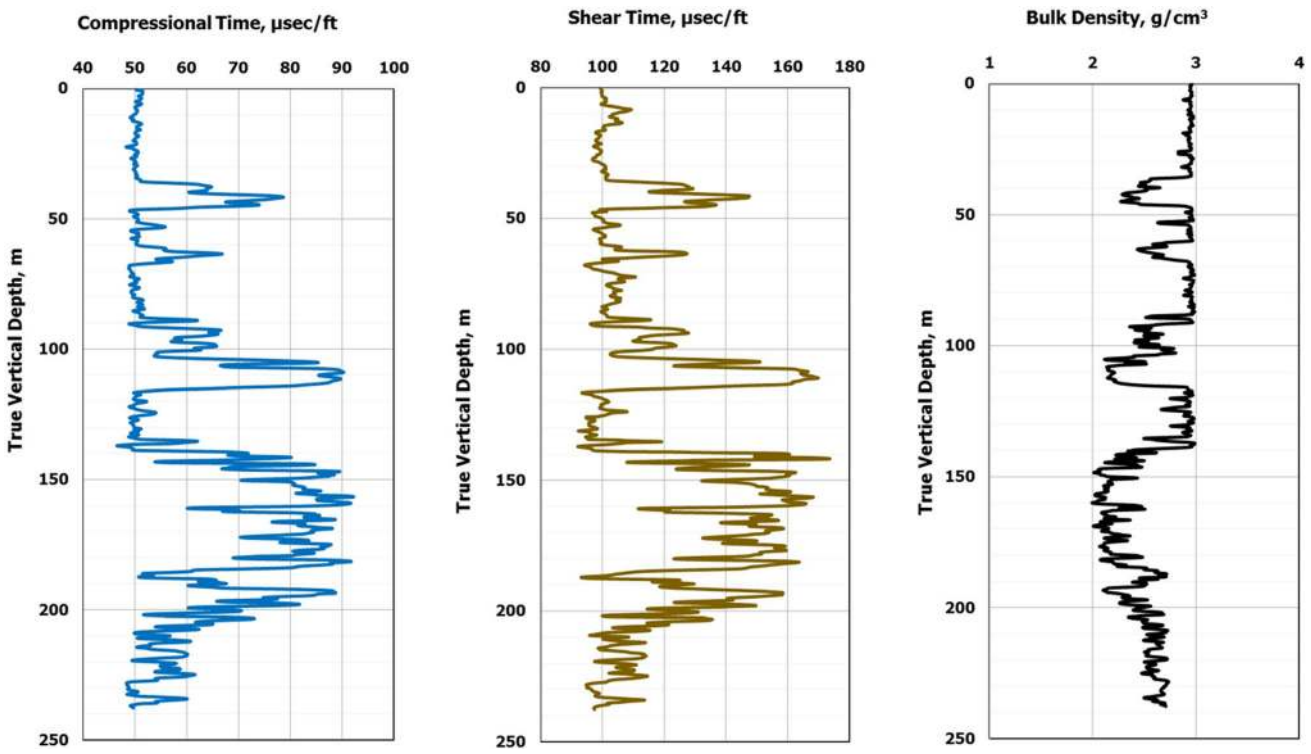

Fig. 10 Log data for case #1. The *top* depth of the formation is represented by the zero value here, and the *bottom* depth is the 237.4 m

modulus. Figure 11a shows that King's correlation (1983) gave a negative value of static Young's modulus which is not acceptable in the upper part of the reservoir, while it became positive and matched the core data in the lower part of the reservoir. Eissa and Kazi equation (1988) underestimated the value of the static Young's modulus. Canady's method (2010) gave static Young's modulus data very close to the dynamic ones without matching the core dat. Wang's correlation (Wang 2000) did not match the core data, while the new method provided an acceptable trend of the Young's modulus that matching the core data. Figure 11b shows that the root-mean-square error has the lowest value (8) when using the developed correlation, while the root-mean-square error was 10.2, 14.7, 15.6, and 30 for King's correlation (King 1983), Wang's correlation (Wang 2000), Canady's method (Canady 2010), and Eissa and Kazi equation (Eissa and Kazi 1988), respectively.

Case #2

Figure 12 shows the log data for case #2; the reservoir section is limestone. For this case, ten values of static Young's modulus obtained from triaxial test are available for matching the estimated values. Figure 13a shows that the new correlation gave the best estimated values of static Young's modulus that matched the core data, while Wang's method (Wang 2000) gave very close values to the new method in the upper part of the reservoir, without matching the core data. Canady's correlation (Canady 2010) overestimated the static Young's modulus values along the whole log interval. Figure 13b shows that the developed correlation gave the lowest mean-square error (7.8) when compare the core static Young's modulus with the predicted one, while the root-means-square error was 15.4 and 16.7 for Wang's correlation (Wang 2000) and Canady's method (Canady 2010), respectively.

Case #3

In this case, a sandstone reservoir with an average porosity of 5–15% with a wide range of grain size and poor sorting was tested using the new correlation. Figure 14 shows the available log data for this reservoir. The new correlation provided the best match of the static values of the available cores, while Canady's correlation (King 1983) showed overestimation for the static Young's modulus. Wang's correlation (Wang 2000) did not match the static Young's modulus value which obtained from the core data as shown in Fig. 15a. The developed correlation gave the lowest root-mean-square error (2.7) for the given 5 core data when comparing with the estimated value from the developed correlation, Fig. 15b. The root-mean-square error was 6.5 and 5.3 for Wang's correlation (Wang 2000) and Canady's method (Canady 2010), respectively, as shown in Fig. 15b.

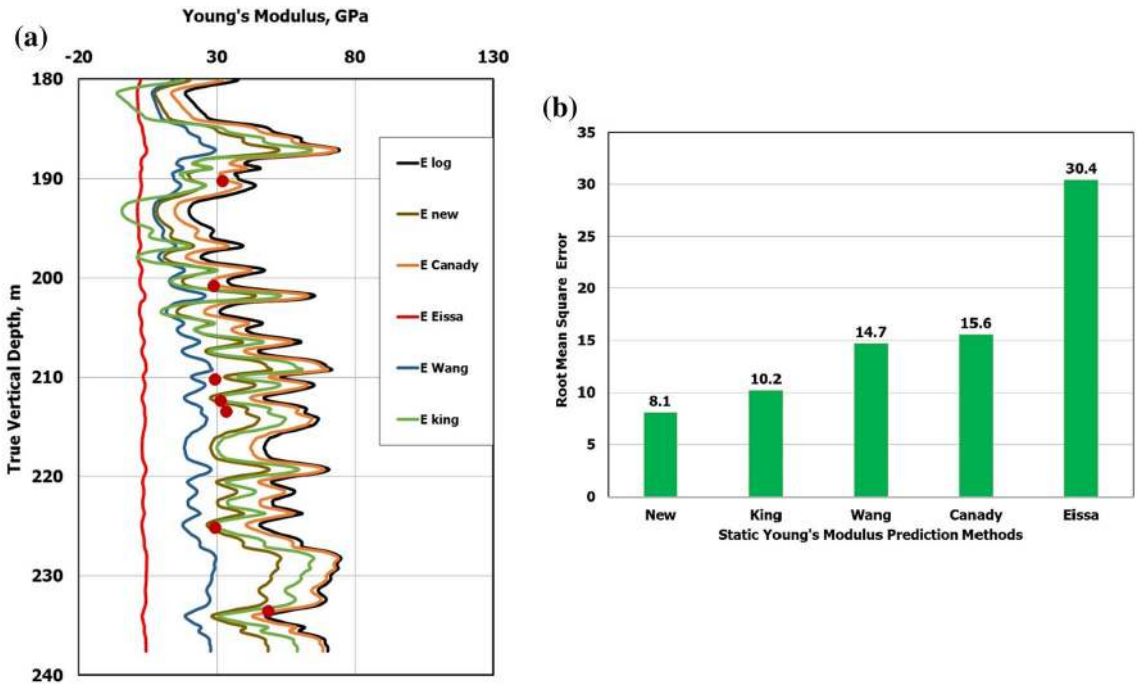

Fig. 11 Estimated Young's modulus value from dynamic one using different correlation, Case #1 limestone formation. E_{new} is the static Young's modulus estimated by the developed correlation, and it gives the best match with the core measured data and lowest RMSE of 8. **a** Prediction of static Young's modulus. **b** Root-mean-square error

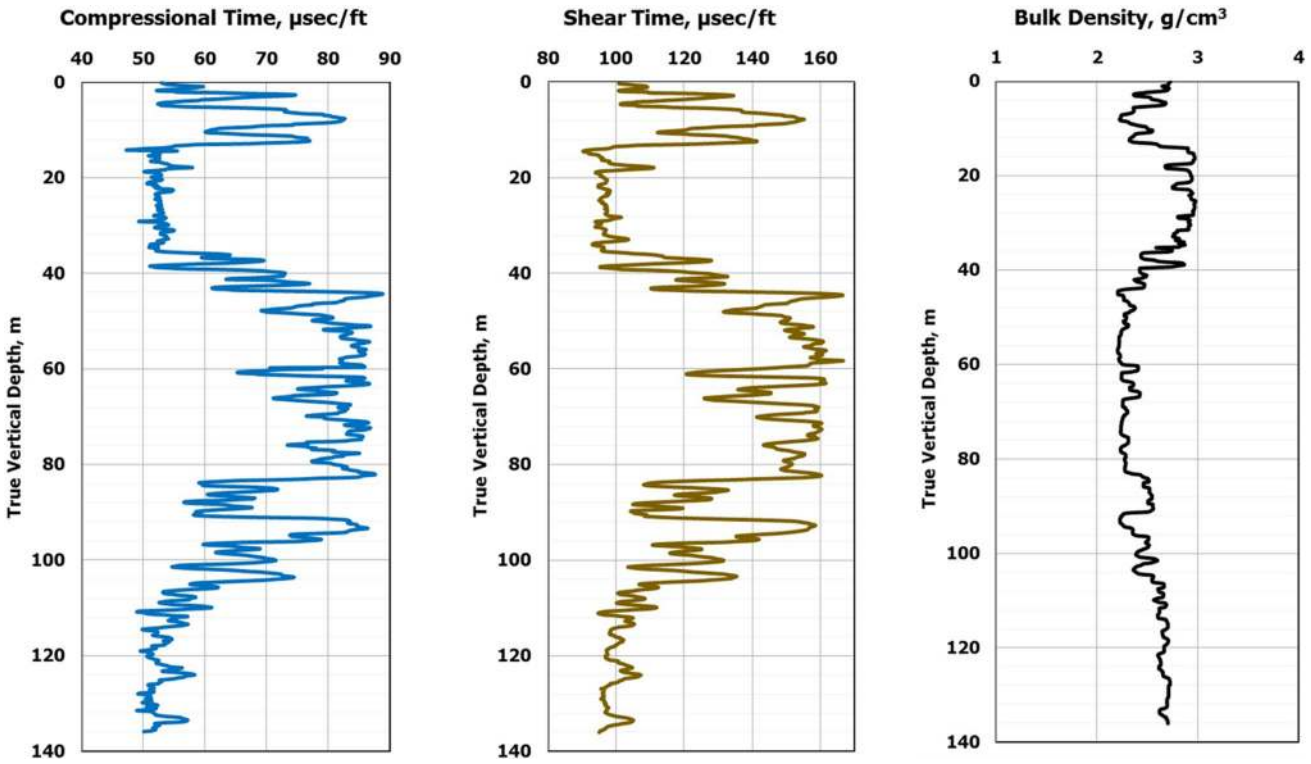

Fig. 12 Log data for case #2 limestone formation. The *top* depth of the formation is represented by the zero value here, and the *bottom* depth is the 136 m

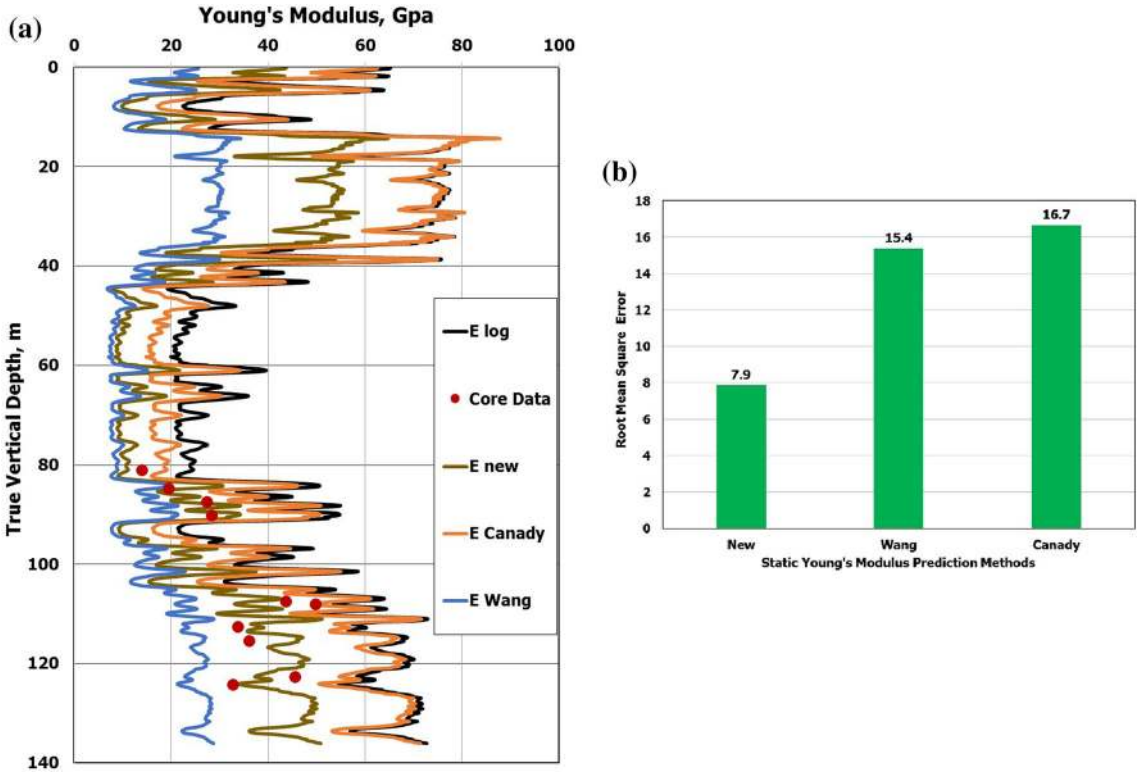

Fig. 13 Estimated Young's modulus value from dynamic one using different correlation, case #2 limestone formation. E_{new} is the static Young's modulus estimated by the developed correlation, and it gives the best match with the core measured data and the lowest root-mean-square error. **a** Prediction of static Young's modulus. **b** Root-mean-square error

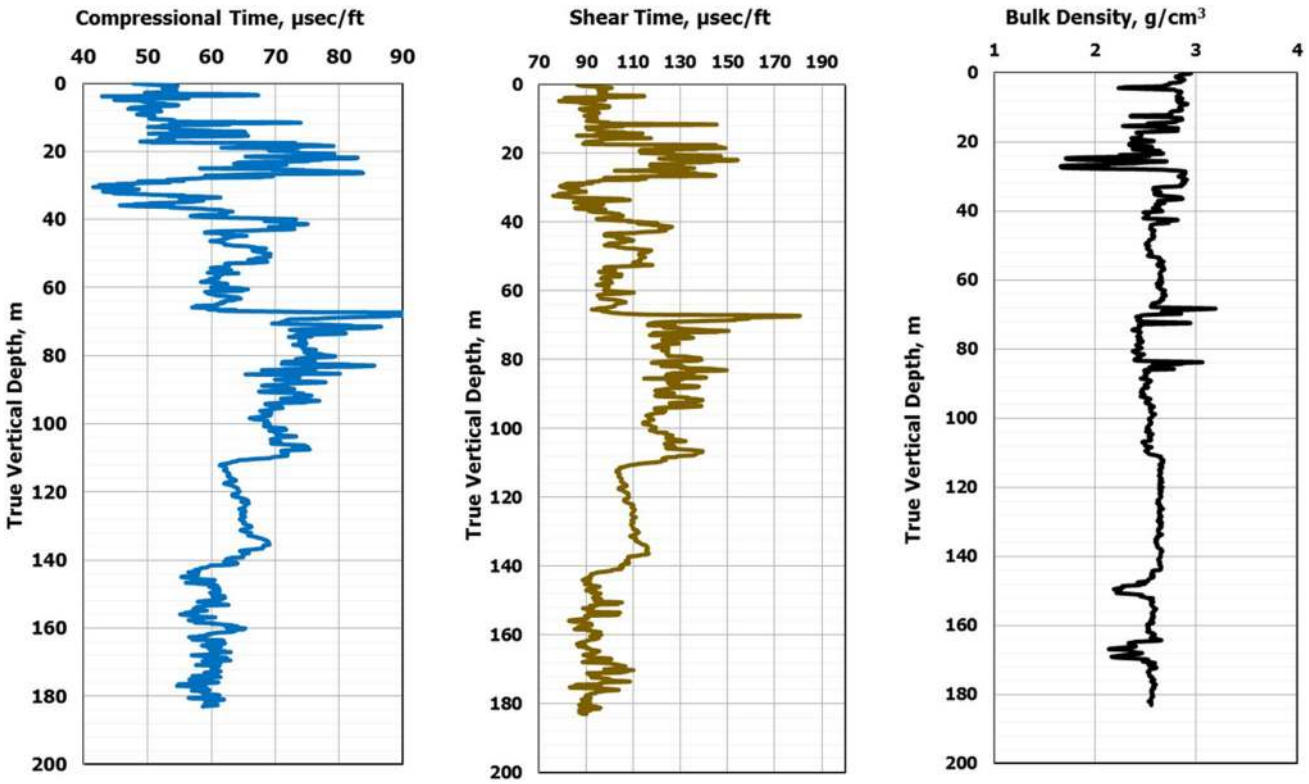

Fig. 14 Log data for case #3 sandstone formation. The *top* depth of the formation is represented by the zero value here, and the *bottom* depth is the 183 m

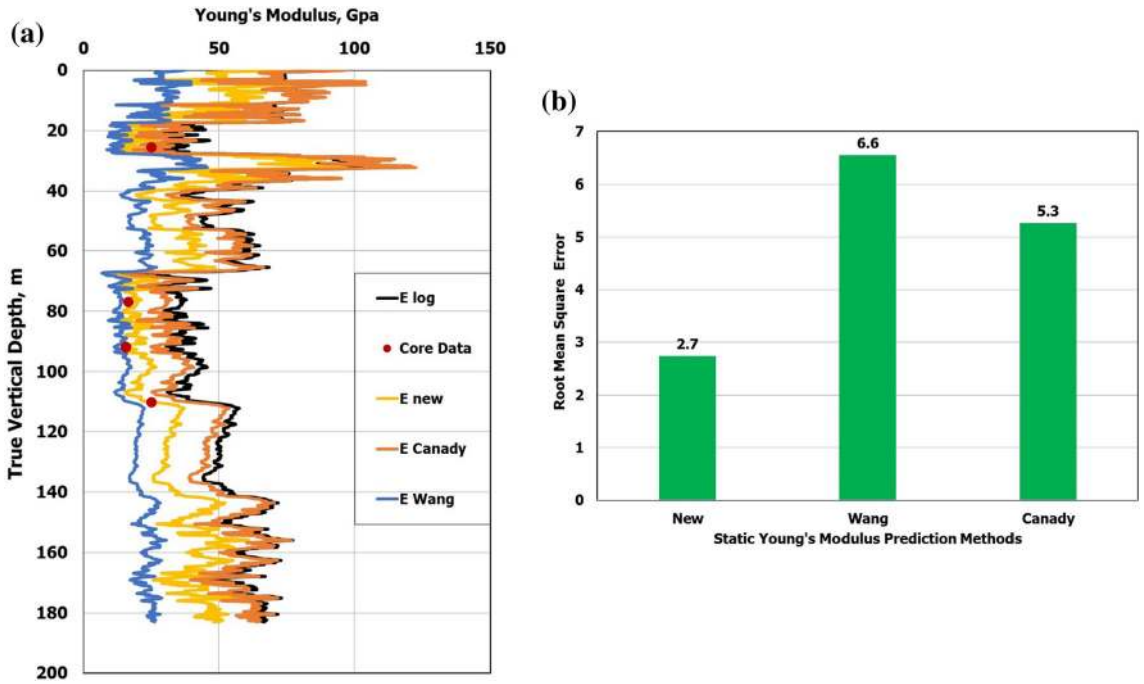

Fig. 15 Estimated Young's modulus value from dynamic one using different correlation, case #3 sandstone formation. E_{new} is the static Young's modulus estimated by the developed correlation, and it gives the best match with the core measured data and the lowest root-mean-square error. **a** Prediction of static Young's modulus. **b** Root-mean-square error

Case #4

Figure 16 shows the available log data for a sandstone reservoir. For this case, only the data for four cores are available for matching the estimated value of static Young's modulus. The new correlation provided the best match compared to previous correlations as shown in Fig. 17a. Wang's method (Wang 2000) underestimated static Young's modulus value, and the values are away for the core data. Canady's correlation (Canady 2010) again overestimated the static Young's modulus values and also did not match the core data. Figure 17b shows that the new correlation gave the lowest root-mean-square error of 9.4, while the root-mean-square error for Wang's correlation (Wang 2000), Canady's method (Canady 2010), and Najibi et al. (Najibi et al. 2015) was 25.2, 11.8, and 15.6, respectively. Based on the results obtained from the previous four cases, it can be concluded that the new correlation provided the best match for the core data with the lowest root-mean-square error as compared with the previous methods.

Importance of using log data to determine static Young's modulus

Several correlations were developed to determine the static Young's modulus based on specific log data. Relying on one or two parameters in the prediction process might lead to wrong estimation of the static Young's modulus. Najibi et al. (Najibi et al. 2015) introduced an empirical correlation to determine the static Young's modulus from compressional velocity (Eq. 11). Using the laboratory measurement from Najibi's correlation has an average absolute error of 20% when used to determine the static Young's modulus comparable to an average absolute error of 14% when using the new developed correlation based on compressional, sonic time, and bulk density, Fig. 18.

$$E_s = 0.169 \times V_p^{3.324} \quad (11)$$

where E_s is static Young's modulus, GPa, and V_p is compressional velocity, Km/s.

Figure 19 shows the static Young's modulus prediction using three methods compared to the core data. The E_{log} method overestimated the static Young's modulus compared to the core data. Najibi's correlation underestimated the static Young's modulus for all core data. Figure 17b shows that the root-mean-square error was 15.6 for Najibi et al. (Najibi et al. 2015) correlation. The new developed correlation yielded very good match for the static Young's modulus compared to the measured laboratory core data. The new developed correlation matched the laboratory data better than other correlations because several log data were considered during the development of this correlation. Figure 9 showed that the relative importance between the static Young's modulus and shear time (or shear velocity) is 57% compared to 28% for the compressional time (velocity).

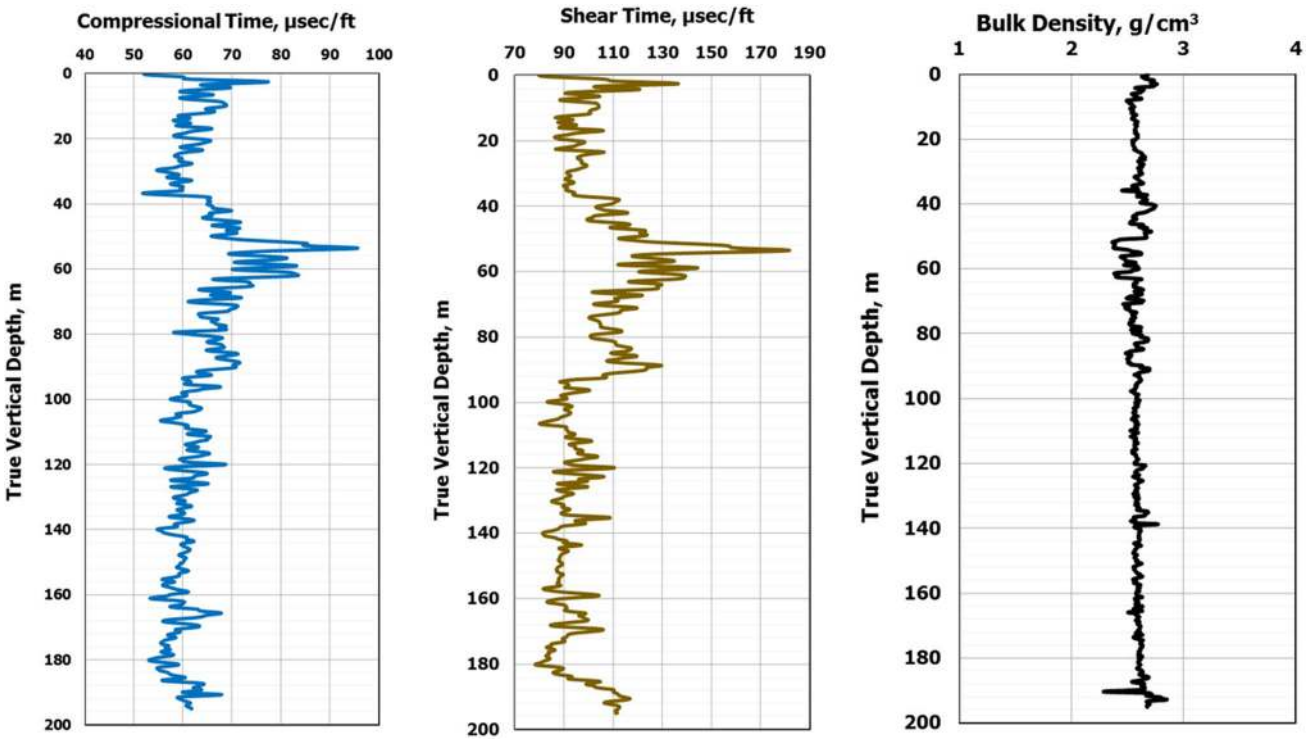

Fig. 16 Log data for case #4 sandstone formation. The *top* depth of the formation is represented by the zero value here, and the *bottom* depth is the 195 m

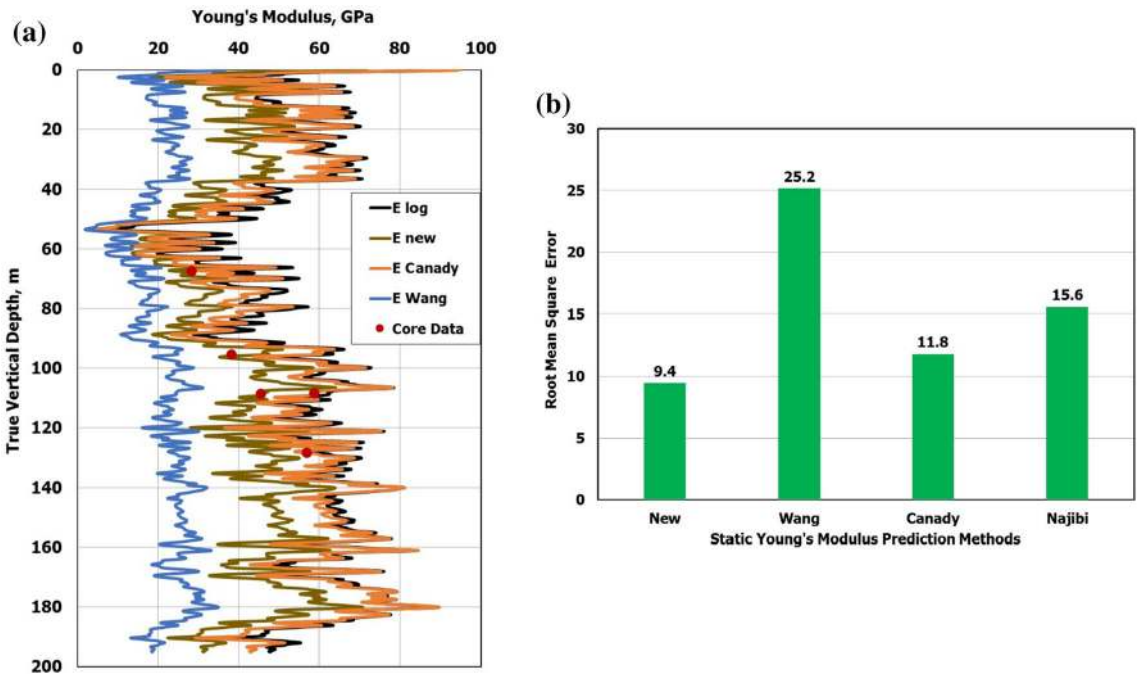

Fig. 17 Estimated Young's modulus value from dynamic one using different correlation, case #4 sandstone formation. E_{new} is the static Young's modulus estimated by the developed correlation, and it gives the best match with the core measured data and the lowest root-mean-square error. **a** Prediction of static Young's modulus. **b** Root-mean-square error

Compressional velocity is very sensitive to gas and fractures, and this will yield wrong values for the compressional velocity logged in gas or fractured formations. Including the shear time (velocity) and bulk density in the prediction of the static Young's modulus will minimize the impact of gas or fractures and that was clear in the good match between the

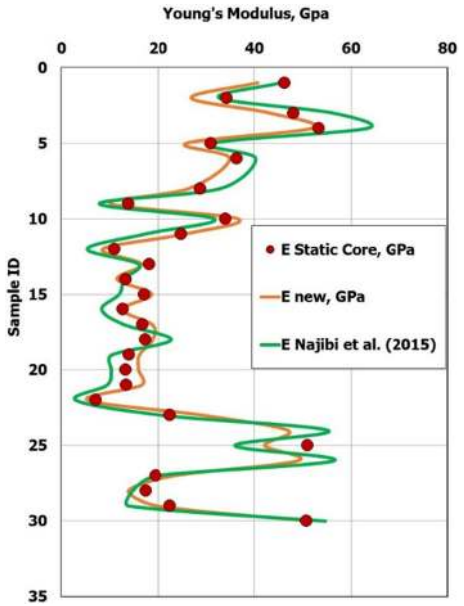

Fig. 18 Comparison between the developed correlation and Najibi et al. (Najibi et al. 2015) correlation on Laboratory data measurements

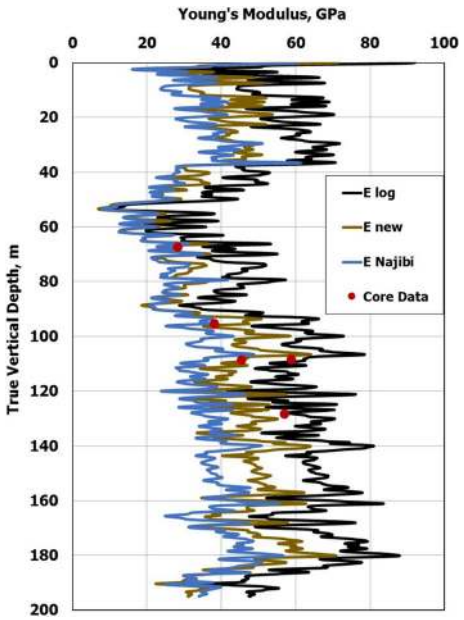

Fig. 19 Comparison between the developed correlation and Najibi et al. (Najibi et al. 2015) correlation on Case 4

static Young's modulus predicted using the new correlations and the ones measured in the laboratory.

Conclusions

In this study, we developed a new correlation that can be used to estimate the static Young's modulus with high accuracy compared to the methods available in the literature. We have conducted regression analysis using more than 600 data points to develop the new correlation. Based on the results obtained, the following conclusions can be drawn:

1. Static Young's modulus can be estimated from the log data directly.
2. The new correlation gave the best match to the static core data in different reservoir types.
3. It gave the lowest root-mean-square error when compare to other methods.

References

Ahmed U, Markley ME, Crary SF (1991) Enhanced in situ stress profiling with microfracture, core and sonic logging data. SPE Forma Eval 6:243–251

Belikov BP, Alexandrov TW, Rysova TW (1970) Elastic properties of rock minerals and rocks. Nauka, Moscow

Brace WF (1965) Relation of elastic properties of rocks to fabric. J Geophys Res 70:5657–5667

Canady WA (2010) Method for full-range young's modulus correction. In: North American unconventional gas conference and exhibition, SPE 143604

Chan MH, Board M (2009) Rock properties and their effect on thermally induced displacements and stresses. J Energy Res Technol 104:384–388

Fan J, Chen, H (2011) Advances in heterogeneous material mechanics. In: International conference on heterogeneous material mechanics, China

Ciccotti M, Mulargia F (2004) Differences between static and dynamic elastic moduli of a typical seismogenic rock. Geophys J Int 157:474–477

Eissa EA, Kazi A (1988) Relation between static and dynamic young's modulus of rocks. Int J Rock Mech Min Sci Geomech 25:479–482

Gorjainov NL (1979) Seismic methods in engineering geology. Nedra, Moscow

Hammam AM, Eliwa M (2013) Comparison between results of dynamic & static moduli of soil determined by different methods. HBRC J 9:144–149

Hardin J, Rocke DM (2005) The distribution of robust distances. J Comput Gr Stat 14:1–19

Howarth DF (1984) Technical note apparatus to determine static and dynamic elastic moduli. Rock Mech Rock Eng 17:255–264

Ide JM (1936) Comparison of statically and dynamically determined young's modulus of rocks. Proc Natl Acad Sci 22:81–92

King MS (1966) Wave velocities in rocks as a function of changes in over burden pressure and pore fluid saturants. Geophysics 31:50–73

King MS (1983) Static and dynamic elastic properties of rocks from the canadian shield. Int J Rock Mech Min Sci 20:237–241

Ledbetter H (1993) Dynamic vs. static young's moduli: a case study. Mater Sci Eng 165:L9–L10

Li J, Guo B, Feng Y (2014) An analytical solution of fracture-induced stress and its application in shale gas exploitation. J Energy Res Technol 136:023102–1: 6

McCann DM, Entwisle DC (1992) Determination of young's modulus of the rock mass from geophysical well logs. Geol Appl Wireline Logs II Geol Soc Spec Publ 65:317–325

Morals RH, Marcinew RP (1993) Fracturing of high-permeability formations: mechanical properties correlations. In: Annual technical conference and exhibition, Houston, Texas, SPE 26561

Najibi AR, Ghafori M, Lashkaripour GR, Asef MR (2015) Empirical relation between strength and static and dynamic elastic properties of Asmari and Sarvak Limestone, two main oil reservoirs in Iran. J Petrol Sci Eng 126:78–82

Nes O, Fjaer E, Tronvoil J, Kristiansen TG, Horsrud P (2012) Drilling Time reduction through an integrated rock mechanics analysis. J Energy Res Technol 134:32802–1: 7

Nguyen VX, Abousleiman YN, Hoang S (2009) Analyses of wellbore instability in drilling through chemically active fractured-rock formations. SPE J 14:283–301

Nur AM, Wang Z (1989) Seismic and acoustic velocities in reservoir rocks. Society of Exploration Geophysicists, Tulsa

Thill RE, Peng SS (1974) Statistical comparison of the pulse and resonance methods for determining elastic moduli. The National Institute for Occupational Safety and Health (NIOSH), NTIS, p 24. https://www.cdc.gov/niosh/nioshtic-2/10009175.html

Walsh JB (1966) Seismic wave attenuation in rock due to friction. J Geophys Res 71:2591–2599

Wang ZN (2000) Seismic and acoustic velocities in reservoir rocks: recent development, vol 3, Society of Exploration Geophysicists, Tulsa

William LF (1969) The variation of young's modulus with rock type and temperature. M.S. Thesis, University of Wisconsin, Madison

Zhou D, Wojtanowicz AK (2002) Analysis of leak-off tests in shallow marine sediments. J Energy Res Technol 124:231–238

Zhou D, Zheng P, Peng J, He P (2015) Induced stress and interaction of fractures during hydraulic fracturing in shale formation. J Energy Res Technol 137:062902–1: 6

Zisman WA (1933) Comparison of the statically and seismologically deter-mined elastic constants of rocks. Proc Natl Acad Sci 19:680–686